Blood-Derived Human iPS Cells Generate Optic Vesicle–Like Structures with the Capacity to Form Retinal Laminae and Develop Synapses

M. Joseph Phillips,[1] *Kyle A. Wallace,*[1] *Sarah J. Dickerson,*[2] *Michael J. Miller,*[2] *Amelia D. Verhoeven,*[1] *Jessica M. Martin,*[1] *Lynda S. Wright,*[1] *Wei Shen,*[1] *Elizabeth E. Capowski,*[1] *E. Ferda Percin,*[3] *Enio T. Perez,*[1] *Xiufeng Zhong,*[4] *Maria V. Canto-Soler,*[4] *and David M. Gamm*[1,5,6]

Purpose. We sought to determine if human induced pluripotent stem cells (iPSCs) derived from blood could produce optic vesicle–like structures (OVs) with the capacity to stratify and express markers of intercellular communication.

Methods. Activated T-lymphocytes from a routine peripheral blood sample were reprogrammed by retroviral transduction to iPSCs. The T-lymphocyte–derived iPSCs (TiPSCs) were characterized for pluripotency and differentiated to OVs using our previously published protocol. TiPSC-OVs were then manually isolated, pooled, and cultured en masse to more mature stages of retinogenesis. Throughout this stepwise differentiation process, changes in anterior neural, retinal, and synaptic marker expression were monitored by PCR, immunocytochemistry, and/or flow cytometry.

Results. TiPSCs generated abundant OVs, which contained a near homogeneous population of proliferating neuroretinal progenitor cells (NRPCs). These NRPCs differentiated into multiple neuroretinal cell types, similar to OV cultures from human embryonic stem cells and fibroblast-derived iPSCs. In addition, portions of some TiPSC-OVs maintained their distinctive neuroepithelial appearance and spontaneously formed primitive laminae, reminiscent of the developing retina. Retinal progeny from TiPSC-OV cultures expressed numerous genes and proteins critical for synaptogenesis and gap junction formation, concomitant with the emergence of glia and the upregulation of thrombospondins in culture.

Conclusions. We demonstrate for the first time that human blood–derived iPSCs can generate retinal cell types, providing a highly convenient donor cell source for iPSC-based retinal studies. We also show that cultured TiPSC-OVs have the capacity to self-assemble into rudimentary neuroretinal structures and express markers indicative of chemical and electrical synapses. (*Invest Ophthalmol Vis Sci.* 2012;53:2007–2019) DOI:10.1167/iovs.11-9313

From the [1]Waisman Center, University of Wisconsin-Madison, Madison, Wisconsin; [2]Cellular Dynamics International, Inc., Madison, Wisconsin; [3]Department of Medical Genetics, Faculty of Medicine, Gazi University, Ankara, Turkey; [4]Wilmer Eye Institute, Department of Ophthalmology, Johns Hopkins University School of Medicine, Baltimore, Maryland; [5]Department of Ophthalmology and Visual Sciences, University of Wisconsin-Madison, Madison, Wisconsin; and [6]Eye Research Institute, University of Wisconsin-Madison, Madison, Wisconsin.

M. V. Canto-Soler did not participate in experiments involving embryonic stem cells.

Supported by the Foundation Fighting Blindness Wynn-Gund Translational Research Acceleration Award; National Institutes of Health Grants R01EY21218, P30HD03352, and 1UL1RR025011 Retina Research Foundation and University of Wisconsin Institute for Clinical and Translational Research; University of Wisconsin Eye Research Institute Kathryn and Latimer Murfee Chair; E. Matilda Ziegler Foundation for the Blind, Inc.; and the Muskingum County Community Foundation. The blood derived iPS cell lines used were obtained at no cost from Cellular Dynamics International, Inc.

Submitted for publication December 13, 2011; revised February 13, 2012; accepted February 15, 2012.

Disclosure: **M.J. Phillips**, None; **K.A. Wallace**, None; **S.J. Dickerson**, None; **M.J. Miller**, None; **A.D. Verhoeven**, None; **J.M. Martin**, None; **L.S. Wright**, None; **W. Shen**, None; **E.E. Capowski**, None; **E.F. Percin**, None; **E.T. Perez**, None; **X. Zhong**, None; **M.V. Canto-Soler**, None; **D.M. Gamm**, Cellular Dynamics International, Inc. (C), P

Corresponding author: David M. Gamm, T609 Weisman Center, University of Wisconsin School of Medicine and Public Health, 1500 Highland Ave, Madison, WI 53705; dgamm@wisc.edu.

Human embryonic stem cells (hESCs) and human induced pluripotent stem cells (hiPSCs) are valuable sources of retinal cell types for in vitro and in vivo studies.[1–10] Unlike hESCs, hiPSCs can be derived from individual patients, and therefore provide a unique opportunity to model retinal degenerative diseases (RDDs),[5,7] perform drug testing,[5,7] and develop autologous cell therapies[7,11]; however, custom application of hiPSC technology to the study and treatment of RDDs requires a convenient supply of donor cells amenable to reprogramming and differentiation along the retinal lineage.

To date, iPSC-based production of neural retina and retinal pigment epithelium (RPE) has been demonstrated only from reprogrammed skin cells[1,4,6,7,12–17] or RPE[18]; however, hiPSCs have been derived from other cell sources as well, including nonmobilized peripheral blood T lymphocytes.[19] The use of T cells for hiPSC reprogramming offers distinct advantages when compared with fibroblasts or keratinocytes. Routine blood draws are less invasive, more likely to maintain sterility, and easier to coordinate than skin biopsies, particularly when working with patients located in remote areas of the world. Furthermore, blood is more commonly banked by cell repositories than fibroblasts, and therefore has greater commercial availability.

In this study, we reprogrammed human T cells activated from a routine peripheral blood mononuclear cell (PBMC) sample to generate iPSCs (termed TiPSCs), and subjected them to our retinal differentiation protocol. As previously shown for hESCs and fibroblast-derived hiPSCs,[7] TiPSCs produced laminar optic vesicle–like structures (OVs) within a developmentally appropriate time window. TiPSC-OVs subsequently gave rise to multiple neuroretinal cell types, including photoreceptor-like

cells, which expressed synapse and gap junction markers at later stages of development. In addition, localized regions of some TiPSC-OVs formed stratified retinal structures, consisting of an outer photoreceptor-like cell layer, an intermediate progenitor cell layer, and an inner retinal ganglion-like cell layer. The innate ability of hiPSC-derived neuroretinal progeny to self-assemble into simple laminae, combined with their capacity for intercellular communication, bodes well for the development of more complex RDD culture models and transplantable tissue-like structures using hiPSC technology.

Materials and Methods

Retrovirus Construction, Production, and Concentration

hiPSCs were generated from activated T cells in collaboration with Cellular Dynamics International's MyCell iPS Cell Services (Madison, WI), based on methods the company previously reported.[19] Briefly, three bicistronic Moloney murine leukemia virus (MMLV) constructs were used to deliver the following pairs of reprogramming genes: (1) *OCT4* and *SOX2*, (2) *c-MYC* and *KLF4*, and (3) *NANOG* and *LIN28*. Retrovirus was generated by polyethylene imine transfection of 293T cells for 4 hours with a combination of plasmids that included the following: an MMLV backbone encoding two reprogramming genes, a GAG-Pol packaging vector, a vesicular stomatitis virus G (VSV-G) pseudotyping vector, and a vector encoding nuclear factor (NF)-κB. The medium was then changed to Dulbecco's modified Eagle's medium (DMEM) with 10% fetal bovine serum and 50 mM HEPES (Invitrogen, Carlsbad, CA). Virus-containing supernatant was collected after 72 hours and filtered. The MMLV was then concentrated 50-fold by volume using AmiconY cassettes (Millipore, Billerica, MA) and centrifuged at 2000*g* for 30 minutes per manufacturer instructions.

T-Cell Activation and Reprogramming

T-cell reprogramming is summarized in Figure 1A. Three milliliters of whole blood from a healthy donor was collected using Vacutainer CPT tubes (BD Biosciences, San Jose, CA). Blood samples were obtained with written informed consent in adherence with the Declaration of Helsinki, and with approval from the institutional review board at the University of Wisconsin-Madison. Following blood sample collection, PBMCs were clarified by centrifugation and frozen. The PBMCs were thawed in AIM-V medium (Invitrogen) and resuspended at a density of 2.0×10^6 cells/mL. T cells within the thawed PBMCs were activated by the addition of OKT3 mAb (10 ng/mL, eBioscience, San Diego, CA) and recombinant human IL-2 (300 U/mL, Peprotech, Rocky Hill, NJ), seeded at 2.0×10^5 cells per well of a 96-well plate, and incubated at 37°C. Two days after activation, the cells were transduced by adding 100 μL of the concentrated MMLV virus cocktail to each well. The virus cocktail was composed of equal parts of each concentrated retrovirus supplemented with 600 U/mL IL-2 and 8 μg/mL polybrene. The 96-well plate was centrifuged at 1000*g* for 90 minutes. After a 2-day incubation, each well of the 96-well plate was transferred to one well of a six-well plate containing irradiated mouse embryonic fibroblasts (MEFs) for 1 week in iPSC medium (DMEM/F12, 20% knockout serum replacement [KOSR], 1% MEM nonessential amino acids, 1 mM L-glutamine, 0.1 mM β-mercaptoethanol [βME], and zebrafish basic FGF [zbFGF, 100 ng/mL]). Then the cells were transitioned to conditioned medium (CM), consisting of iPSC medium without zbFGF that was conditioned on MEFs for 8 days, filtered, and supplemented with zbFGF thereafter. Colonies with morphology similar to iPSC colonies were readily visible between day 17 and day 20 after transduction. True iPSC colonies in the reprogramming wells were identified by morphology and live-cell staining with Tra-1-60 antibody. The identified iPSC colonies were hand-picked and propagated using iPSC medium on an MEF feeder layer.

Human Pluripotent Stem Cell Maintenance Culture

hESCs (H9/WA09 line obtained from WiCell, Madison, WI) and iPSCs (TiPSC-5 and the fibroblast-derived IMR90-4 line) were maintained on MEF feeder layers. hESCs were grown in hESC medium, which was identical to iPSC medium with the exception of the concentration of bFGF used (4 ng/mL for hESC medium versus 100 ng/mL for iPSC medium). Morphologically identifiable differentiated cells were mechanically removed, and cells were passaged every 5 to 6 days.

Targeted Retinal Differentiation of Human Pluripotent Stem Cells

Cells were differentiated to a retinal cell fate according to our previously established protocol.[6,7] Briefly, cell colonies were enzymatically lifted from MEF with dispase (1 mg/mL) and grown as aggregates in suspension for 4 days in embryoid body (EB) medium containing DMEM/F12, 20% KOSR, 1% MEM nonessential amino acids, 1 mM L-glutamine, and 0.1 mM βME. Next, EB medium was replaced with neural induction medium (NIM) containing DMEM/F12, 1% N2 supplement, MEM nonessential amino acids, and 2 μg/mL heparin. Suspended cell aggregates were grown in NIM for 2 days and then transferred to laminin-coated plates where they reattached to the culture dish and were grown for an additional 10 days in NIM. At day 16, the loosely adherent central portions of the neural clusters were lifted from the plate with mechanical trituration. These neural clusters formed free-floating spherical aggregates in retinal differentiation medium (RDM) containing DMEM/F12 (3:1), 2% B27 supplement (without retinoic acid), MEM nonessential amino acids, and penicillin-streptomycin. At day 20 of differentiation, OVs were isolated and separated from forebrain neurospheres based on their distinctive appearances under light microscopy, as reported earlier.[7] For RPE generation, neural rosettes were maintained in adherent cultures (i.e., not mechanically lifted) and differentiated in RDM as previously reported.[6,7]

DNA Fingerprinting, Karyotype, and Teratoma Analysis

Genomic DNA was isolated from TiPSCs and the donor PBMCs using the DNeasy Blood and Tissue kit (Qiagen, Valencia, CA). The samples were sent to Cell Line Genetics (Madison, WI) for short tandem repeat (STR) analysis. Genotypes for 15 STR loci were analyzed between PBMCs and TiPSCs. G-banding karyotype analysis was conducted by Cell Line Genetics. Teratoma analysis was performed by WiCell as previously described.[19]

Live Cell Immunocytochemistry

Tra-1-60 live-cell immunocytochemistry was performed by incubating cells with 10 μg of Tra-1-60 primary antibody (MAB4770, R&D Systems, Minneapolis, MN) for 1 hour, washing with DMEM/F12, and then incubating with 1:100 dilutions of IgM AlexaFluor488-conjugated secondary antibody (Invitrogen) for 30 minutes. Tra-1-60–positive colonies were visualized by fluorescent microscopy and mechanically isolated for propagation.

Fixed Cell Immunocytochemistry

Immunocytochemistry was performed as previously reported.[6] Briefly, OVs were partially dissociated by trituration and plated for up to 1 week on polyornithine- and laminin-coated coverslips and fixed in 4% paraformaldehyde for 30 minutes. For experiments examining laminar structure, free-floating OVs were fixed and cryosectioned. Coverslips containing cell clusters or sections were placed in blocking solution (10% normal donkey or goat serum and 0.5% triton-x in PBS) for 1 hour and incubated overnight at 4°C with primary antibodies (Supplemental Table 1; supplemental material is available at: http://www.iovs.org/

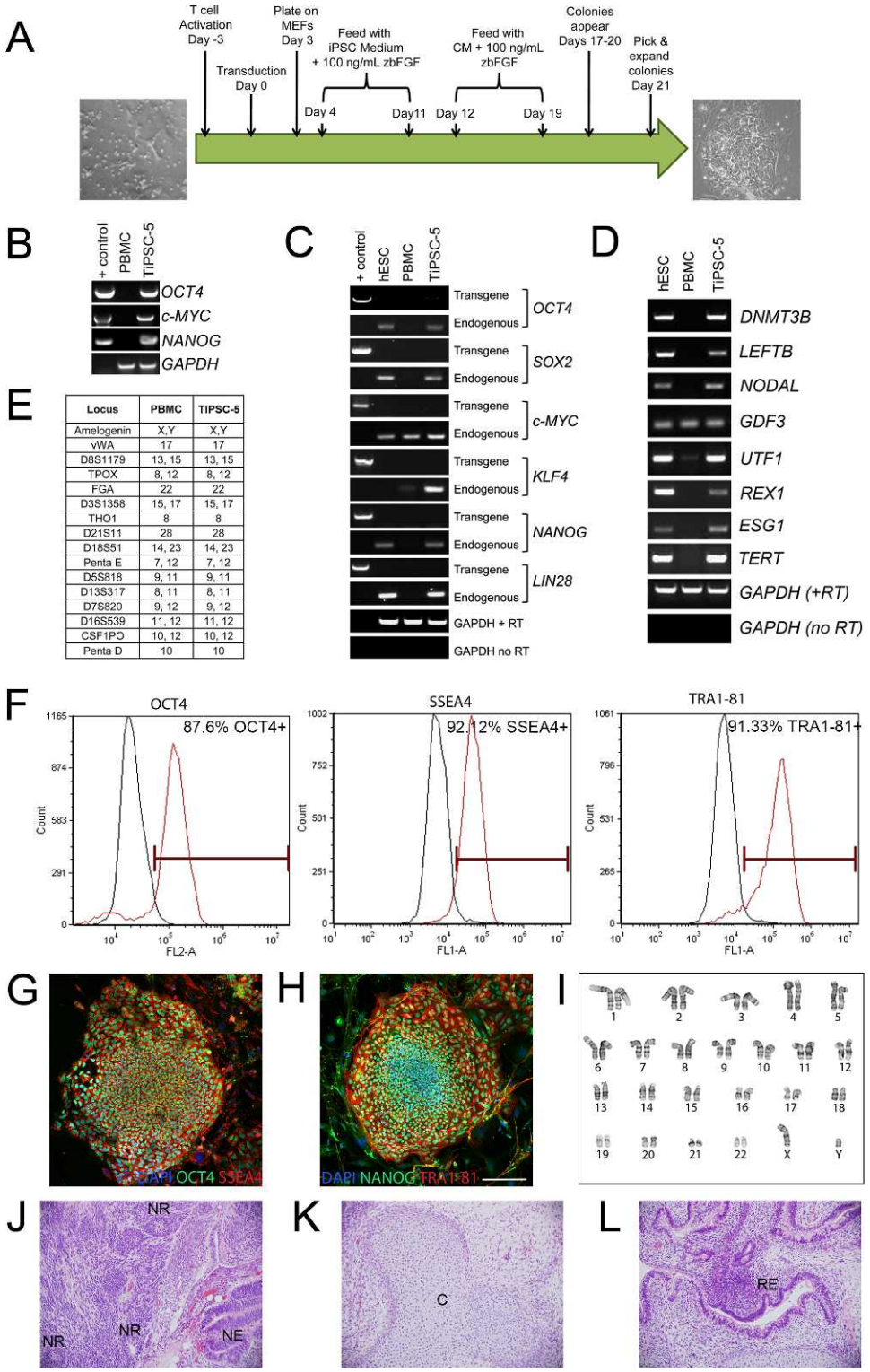

Locus	PBMC	TIPSC-5
Amelogenin	X,Y	X,Y
vWA	17	17
D8S1179	13, 15	13, 15
TPOX	8, 12	8, 12
FGA	22	22
D3S1358	15, 17	15, 17
THO1	8	8
D21S11	28	28
D18S51	14, 23	14, 23
Penta E	7, 12	7, 12
D5S818	9, 11	9, 11
D13S317	8, 11	8, 11
D7S820	9, 12	9, 12
D16S539	11, 12	11, 12
CSF1PO	10, 12	10, 12
Penta D	10	10

Figure 1. Derivation and characterization of TiPSCs. (**A**) Schematic diagram depicting the steps involved in reprogramming activated human T cells to TiPSCs. (**B**) Genomic DNA PCR analysis revealed the genomic integration of the reprogramming vectors in the TiPSC-5 line (one reprogramming gene from each bicistronic vector was evaluated). Reprogramming vector plasmids were used as a positive control; no products were seen in the initial PBMC population. (**C**) RT-PCR analysis demonstrated the silencing of reprogramming transgenes and activation of endogenous pluripotency genes in TiPSC-5. Endogenous gene expression in TiPSC-5 was similar to that found in the H9 (WA09) hESC line. Glyceraldehyde-3-phosphate dehydrogenase was used as a normalizing control, whereas a PCR reaction lacking reverse transcriptase verified the absence of genomic DNA contamination. (**D**) RT-PCR analysis revealed expression of pluripotency genes in TiPSC-5 cells, which was comparable with H9 hESCs. Only *GDF3* was expressed in PBMCs. (**E**) Analysis of 15 STR loci and Amelogenin demonstrated shared genetic identity of the parent PBMCs and TiPSC-5 cells. (**F**) The vast majority of TiPSCs expressed the pluripotency markers OCT4, SSEA-4, and TRA1-81, as shown by flow cytometry. (**G, H**) Immunocytochemistry analysis confirmed expression of pluripotency markers in TiPSC-5 colonies. Scale bar = 100 μm. (**I**) TiPSC-5 displayed a normal karyotype and (**J, K**) teratoma analysis revealed the presence of tissue from all three developmental germ layers: (**J**) ectoderm (NR, neural rosettes; NE, neural epithelium), (**K**) mesoderm (C, cartilage), and (**L**) endoderm (RE, respiratory/gut epithelium).

lookup/suppl/doi:10.1167/iovs.11–9313/-/DC) diluted in blocking solution. Cells were then washed and incubated with secondary antibodies diluted in blocking solution for 30 minutes at room temperature. Cells were imaged on a Nikon 80i laser scanning confocal microscope (Nikon Corp., Tokyo, Japan).

RT-PCR and Quantitative RT-PCR

Total RNA for each sample was prepared using the RNeasy Mini Plus Kit (Qiagen), genomic DNA was removed with DNase I, and first-strand cDNA was synthesized using the iScript cDNA Synthesis Kit (Biorad, Hercules, CA) or the Improm II Reverse Transcription Kit (Promega, Madison, WI). RT-PCR to analyze transgene and endogenous mRNA expression in iPSCs was carried out using primers previously described.[20,21] All other primers were designed using Primer3 software and are listed in Supplemental Table 2. RT-PCR was performed with GoTaq PCR master mix (Promega) and subsequent PCR products were run on 2% agarose gels. For quantitative RT-PCR (qRT-PCR), reactions were performed with Sybr Green Supermix (Applied Biosystems, Carlsbad, CA) and an Applied Biosystems 7500 qRT-PCR machine. RT-PCR reactions were run at either 30 or 35 cycles, and all qRT-PCR reactions were run at 40 cycles. qRT-PCR statistical analysis was performed with the Relative Expression Software Tool program (Qiagen).

Genomic DNA PCR

Total cellular DNA was isolated using the DNeasy Blood and Tissue Kit (Qiagen), according to manufacturer instructions. PCR to detect integration of the reprogramming vectors was performed using primers previously described.[20,21]

Flow Cytometry Analysis

TiPSCs were harvested, stained for the presence of Tra-1-81 (488 Dylight-conjugated TRA-1–81; Millipore) and stage-specific embryonic antigen 4 (SSEA-4) (FITC-conjugated clone MC813-70; BD Pharmingen, San Diego, CA) for 30 minutes, and then washed and analyzed. Intracellular octamer-binding transcription factor (OCT)3/4 (phycoerythrin-conjugated clone 40/OCT-3; BD Pharmingen) immunostaining was performed overnight on cells fixed with 2% paraformaldehyde and permeabilized with PBS + 0.1% saponin. Analysis for these experiments was performed using an Accuri flow cytometer (Accuri Cytometers, Ann Arbor, MI) and FCS Express version 3 (De Novo Software, Los Angeles, CA). For experiments involving CHX10 (VSX2), cells were dissociated with trypsin, washed, and fixed with 0.1% paraformaldehyde for 10 minutes. Cells were incubated overnight in 1 μg CHX10 antibody per 1 million cells in fluorescence-activated cell sorting (FACS) buffer. Cells were then incubated with Alexa488 secondary antibodies for 2 hours, washed, and sorted with a BD FACSCaliber (BD Biosciences, Franklin Lakes, NJ). CHX10 data were analyzed with CellQuest Pro software (BD Pharmingen). For all experiments, dead cells stained by propidium-iodide were excluded from the analysis and isotype antibodies (BD Pharmingen) were used as controls.

Results

Generation and Characterization of TiPSCs

Activated T cells from 3 mL of whole blood were reprogrammed to iPSCs via a single transduction of a cocktail of three bicistronic MMLV vectors, each encoding two reprogramming genes. After transduction, cells were plated on MEF feeder layers, cultured with iPSC medium for 1 week, and then transitioned to MEF CM. After culturing in CM for an additional week, the pluripotency status of each colony was assessed by live-cell staining of the ESC surface marker, Tra-1-60 (data not shown). Colonies that stained with Tra-1-60 and had iPSC-like morphology were picked and expanded. The steps involved in the generation of TiPSC line 5 (TiPSC-5) are summarized in Figure 1A.

The TiPSC-5 line was extensively characterized for pluripotency and genetic identity. Genomic DNA PCR analysis using transgene-specific primers verified the integration of each bicistronic reprogramming vector in the TiPSC-5 line (Fig. 1B). Although transgene expression is essential for the initial reprogramming event in iPSC derivation, transgenes are typically silenced and their endogenous counterparts are upregulated. This switch was documented by RT-PCR in the TiPSC-5 line (Fig. 1C). TiPSC-5 also expressed a number of genes not included in the reprogramming vectors that are typical of pluripotent stem cells (Fig. 1D). Pluripotency gene expression patterns in TiPSC-5 closely matched those found in hESCs, whereas most pluripotency genes were not expressed in the initial PBMC population (Figs. 1C, 1D). Comparison of STRs between the donor PBMCs and the TiPSC-5 line revealed no differences, confirming their shared identity (Fig. 1E). Flow cytometry analysis and immunocytochemistry showed that the vast majority of TiPSC-5 cells expressed the pluripotency markers SSEA-4, Tra-1-81, OCT4, and NANOG (Figs. 1F–H). TiPSC-5 cells had a normal karyotype (Fig. 1I), and teratoma analysis confirmed the ability of this line to differentiate into cells belonging to all three developmental germ layers (Figs. 1J–L).

Differentiation of TiPSCs to a Primitive Anterior Neuroepithelial Cell Fate

TiPSC-5 cells were differentiated to a primitive anterior neuroepithelial cell fate using a protocol established previously.[6,7] Pluripotent colonies were lifted and placed in suspension culture to generate free-floating EBs (Fig. 2A). Six days later, TiPSC-EBs were plated onto laminin-coated plastic, whereupon they formed tightly packed neural colonies by day 16 (Fig. 2B, dashed outline), identical to those derived from hESCs and fibroblast-derived hiPSCs.[6,7] Similarly, between day 4 and day 16, differentiating TiPSC-EBs upregulated many transcription factors involved in anterior neuroepithelial development and/or eye field specification, including *SIX3*, *SIX6*, *OTX2*, *LHX2*, *PAX6*, and *MITF* (Fig. 2C). *PAX6* expression appeared as a doublet band, representing the +5a and −5a isoforms, consistent with previous results obtained using the H9 hESC line.[6] As early as day 10, most cells within the tightly packed neural colonies expressed the transcription factors LHX2, PAX6, SIX3, SIX6, and OTX2 (Figs. 2D–O).

Expression of anterior neuroepithelial/eye field specification genes at day 10 was compared among the TiPSC-5 line, the IMR90-4 fibroblast-derived hiPSC line, and the H9 hESC line (Fig. 2P). Using the same differentiation protocol, quantitative RT-PCR analysis showed no significant differences in the expression of *SIX3*, *SIX6*, *PAX6*, *RX*, and *LHX2* between the TiPSC-5 and H9 lines ($n = 3$ for each cell line). Only *OTX2* showed a significant change, although the relative reduction in expression in TiPSC-5 was modest (0.514-fold change, $P < 0.001$). IMR90-4 and H9 gene expression did not differ significantly. These results demonstrate that hESCs, fibroblast-derived hiPSCs, and TiPSCs can differentiate to the earliest stages of retinogenesis in a similar manner.

Isolation of OVs from TiPSCs

Recently, we demonstrated that three-dimensional OVs could be cultured from hESCs and fibroblast-derived hiPSCs.[7] These distinctive laminar structures, which contained a highly enriched population of neuroretinal progenitor cells (NRPCs), were mechanically isolated from forebrain progenitor neurospheres, pooled, and further differentiated in culture.[7] In the

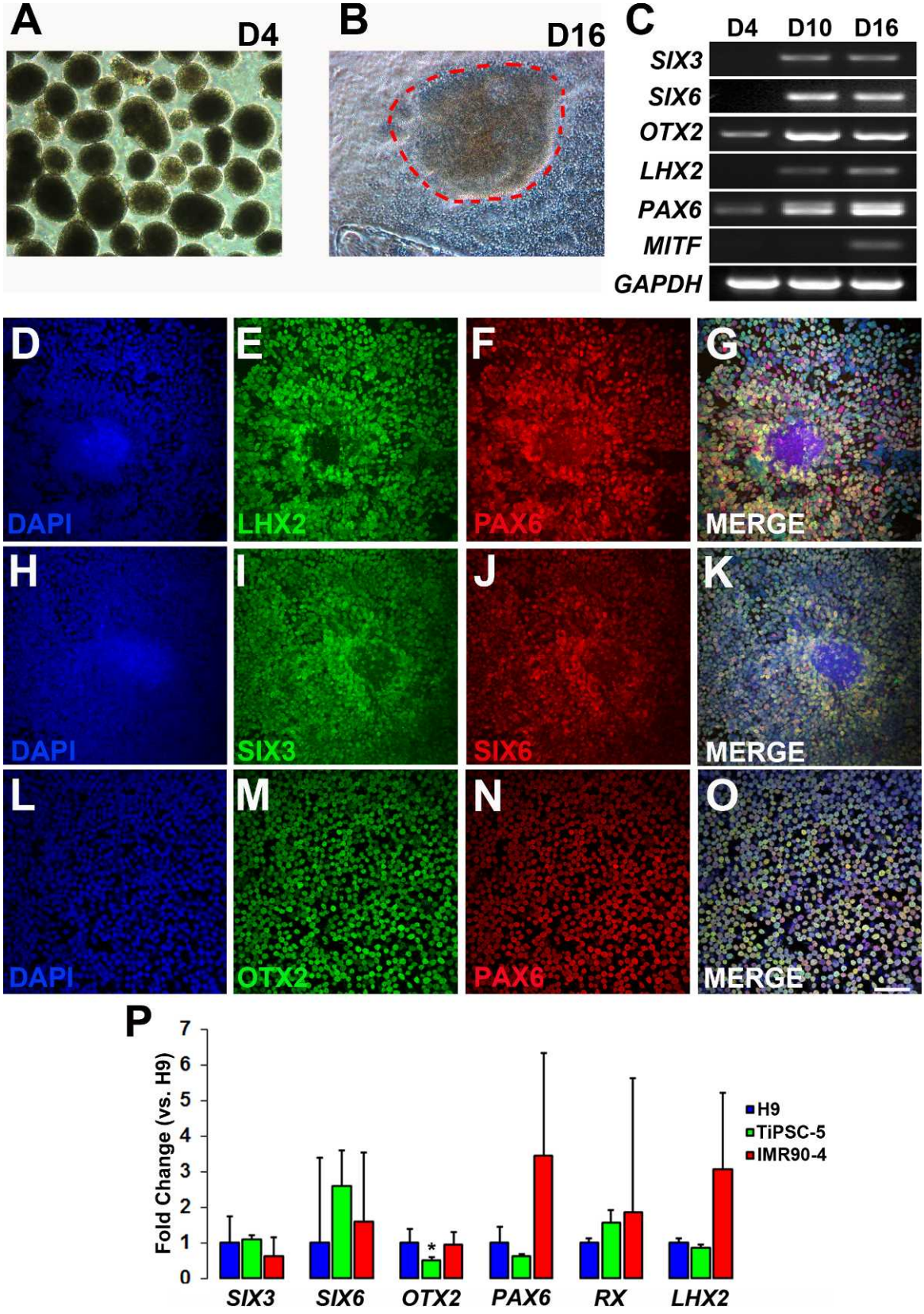

Figure 2. Anterior neuroepithelium/eye field specification of TiPSCs. (**A**) Lifted pluripotent TiPSC-5 colonies formed EBs (day 4 pictured). (**B**) Subsequent plating and culturing of EBs led to the formation of tightly packed colonies of neural cells (dashes; day 16 pictured). (**C**) RT-PCR demonstrated upregulation of anterior neuroepithelium/eye field specification genes at day 4, day 10, and day 16. (**D–O**) Immunocytochemistry analysis of plated EBs on day 10 of differentiation revealed that most cells expressed (**E**) LHX2, (**F, N**) PAX6, (**I**) SIX3, (**J**) SIX6, and (**M**) OTX2 (**D**, **H**, **L** = DAPI). Merged images confirmed co-expression of (**G**) LHX2 and PAX6, (**K**) SIX3 and SIX6, and (**O**) OTX2 and PAX6. Scale bar = 50μm (applies to panels D–O). (**P**) qRT-PCR was used to compare gene expression at day 10 between H9 hESCs, TiPSC-5, and a commonly used fibroblast-derived hiPSC line, IMR90-4. Results were normalized to H9 hESC gene expression. Only *OTX2* expression was significantly different between the TiPSC-5 and H9 lines (0.54-fold less expression in the former, $P < 0.001$). Error bars depict standard error of the mean.

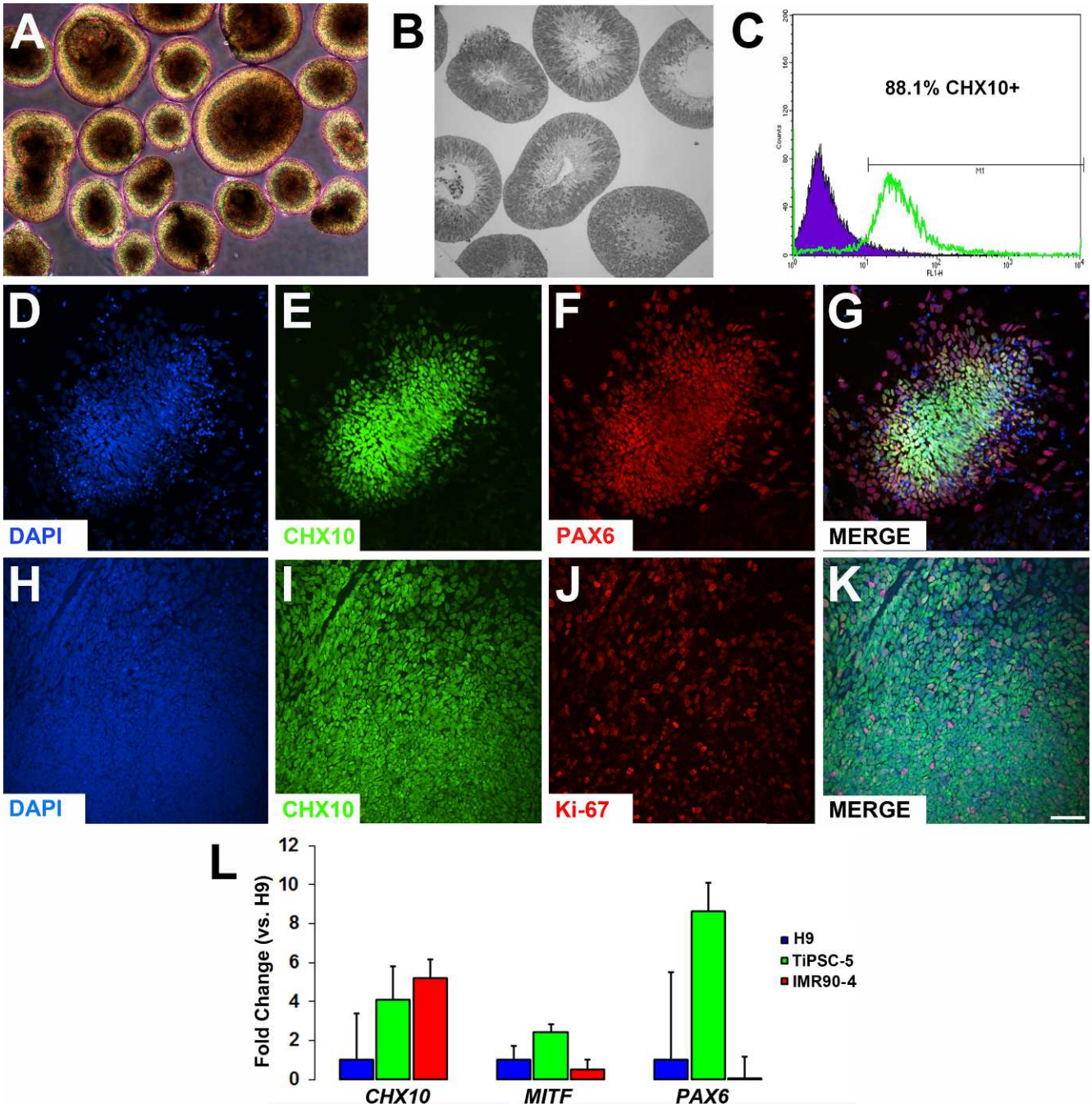

Figure 3. Generation and isolation of TiPSC-OVs expressing neuroretinal progenitor cell markers. (**A**) Phase-contrast micrograph of mechanically isolated and pooled OVs at day 20, which were easily identified by their phase bright outer mantle of radially oriented cells. (**B**) Plastic embedded section of TiPSC-OVs counterstained with toluidine blue, showing cell nuclei confined mainly to the outer mantle, along with an inner cytoplasmic layer that often surrounded a hollow center. (**C**) Most cells in isolated TiPSC-OVs expressed the neuroretinal progenitor marker CHX10 (88.1%) at day 20, as shown by FACS analysis. (**D–K**) Immunocytochemistry analysis of partially dissociated and plated TiPSC-OVs at day 20 demonstrated expression of (**E, I**) CHX10, (**F**) PAX6, and (**J**) Ki67 (**D, H** = DAPI). (**G**) Most cells co-expressed CHX10 and PAX6, particularly in the center of the plated clusters. (**K**) Co-expression of CHX10 and Ki67 further revealed that the neuroretinal progenitors were mitotically active. Scale bar = 50 μm (applies to **D–K**). (**L**) qRT-PCR gene expression analysis showed no significant differences in the expression of *CHX10*, *MITF*, or *PAX6* between OVs derived from the H9 hESC line and the TiPSC-5 or IMR90-4 lines at day 20. Error bars depict standard error of the mean.

present study, we sought to determine whether the TiPSC-5 line also produced OVs.

At day 16 of our differentiation protocol, the tightly packed neural colonies (Fig. 2B) were lifted and grown as free-floating spherical aggregates. By day 20, 61.2% ± 8.4% (n = 4) of these aggregates formed OVs that were identical to those obtained from hESCs or fibroblast-derived hiPSCs.[7] By comparison, WA01 hESCs formed 40.70% ± 9.74% OVs and WA 09 hESCs produced 20.40% ± 4.30% (WA09 was reported previously).[7] TiPSC-OVs were readily identifiable under light microscopy amidst their non-OV counterparts by virtue of their phase-bright outline and radial distribution of cells, which surrounded a dark, often acellular core. TiPSC-OVs were mechanically separated from non-OV neurospheres to yield pure OV cultures

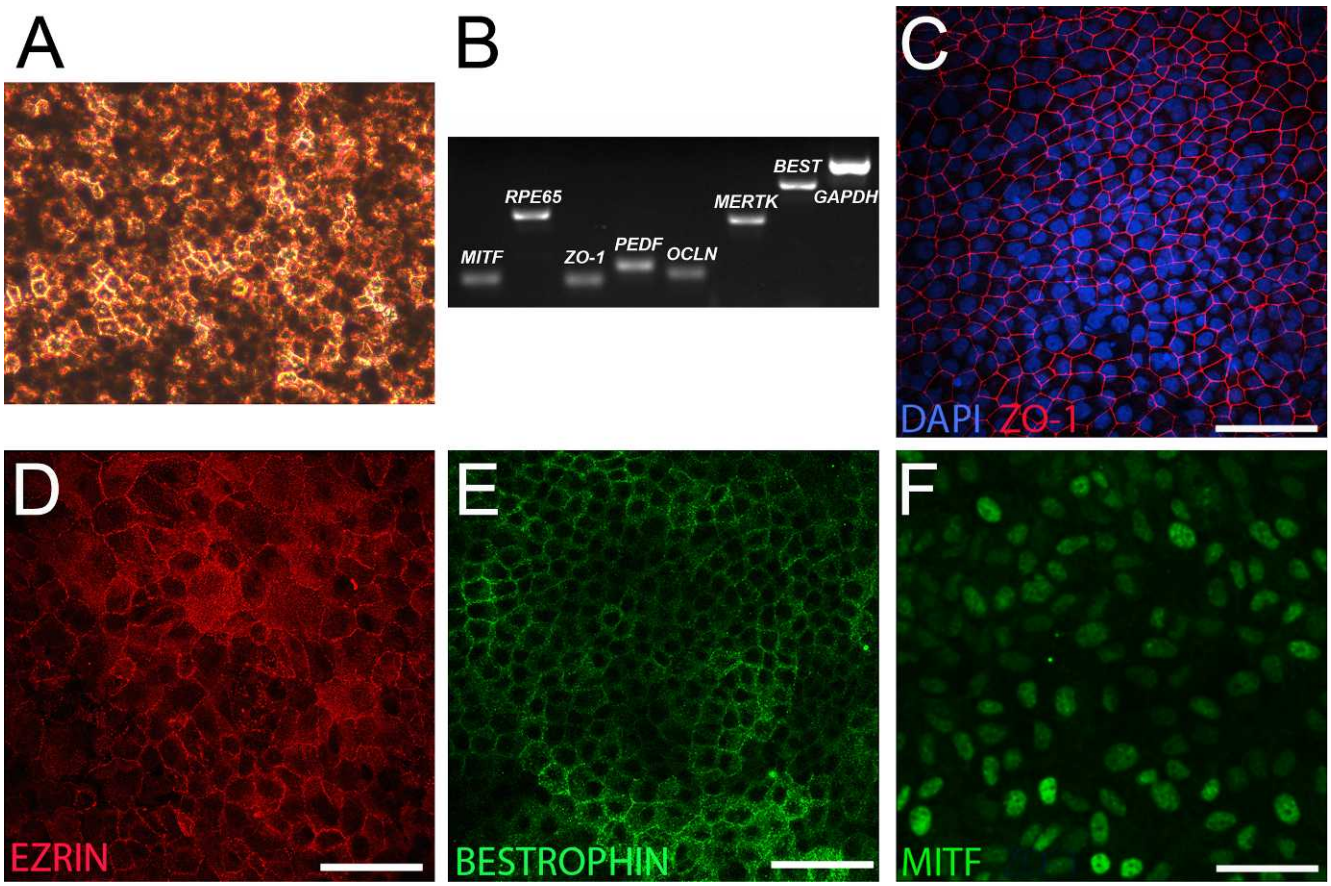

Figure 4. Differentiation of RPE-like cells from plated TiPSC cultures. (**A**) Phase micrograph showing a tightly packed monolayer of heavily pigmented cells with a polygonal morphology (day 105 pictured). (**B**) RT-PCR analysis at day 60 confirmed expression of genes characteristic of RPE. (**C–F**) Immunocytochemistry analysis demonstrated expression of (**C**) ZO-1, (**D**) EZRIN, and (**E**) BESTROPHIN at day 66. (**F**) MITF was also uniformly expressed in RPE-like cells (day 49 pictured). Scale bars = 50 μm.

(Fig. 3A). Plastic-embedded sections counterstained with toluidine blue further highlighted the ordered arrangement of nuclei, which were located around the outer portion of TiPSC-OVs (Fig. 3B).

TiPSC-OVs were analyzed at day 20 for expression of markers indicative of NRPCs. FACS analysis indicated that the vast majority of cells within TiPSC-OVs expressed CHX10 (VSX2), a marker for NRPCs (88.1%; Fig. 3C). Furthermore, immunocytochemistry analysis of partially dissociated and plated TiPSC-OVs showed extensive co-expression of CHX10 with the transcription factor PAX6 (Figs. 3D–G) and the cell proliferation marker Ki-67 (Figs. 3H–K). Last, gene expression of *CHX10*, *MITF*, and *PAX6* in TiPSC-OVs was compared with that of H9 hESC-OVs and IMR90-4 hiPSC-OVs using qRT-PCR (Fig. 3L). Although TiPSC-OVs showed similar or higher expression of each of these genes relative to the other lines, none of the differences reached statistical significance (n = 3 for each cell line).

Generation of RPE from TiPSCs

As described previously using hESCs and fibroblast-derived hiPSCs, OVs produced by TiPSCs rarely yielded RPE under our standard culture conditions[7]; however, when TiPSC-EBs were left plated at day 16 and grown in RDM, rather than being mechanically lifted to form free-floating OVs, extensive sheets of cells acquired an RPE phenotype. Beginning between day 40 and day 50, discrete patches of cells acquired a polygonal morphology and became increasingly pigmented over time (Fig. 4A). These pigmented patches of RPE-like cells were microdissected and analyzed by RT-PCR, which revealed expression of signature RPE genes, such as *MITF*, *RPE65*, *ZO-1*, *PEDF*, *OCCLUDIN*, *MERTK*, and *BESTROPHIN* (Fig. 4B). Immunocytochemical analysis confirmed expression of ZO-1 (Fig. 4C), EZRIN (Fig. 4D), BESTROPHIN (Fig. 4E), and MITF (Fig. 4F).

Generation of Retinal Neurons from TiPSC-OVs

Most nonphotoreceptor neuroretinal markers are only cell-specific within the retina itself, owing to their expression elsewhere in the central nervous system. Our OV culture system, however, allows us to track retinal neuron development with a high level of certainty, as all progeny arise from a highly enriched NRPC population.[7] To examine the generation of particular neuroretinal cell types, TiPSC-OVs were partially dissociated, plated onto laminin-coated coverslips, and cultured for several days to allow cell migration and neuronal process extension. Cells were then fixed and examined by immunocytochemistry. By 39 days of total differentiation, retinal neurons expressing HUc/d and TUJ1 were prevalent in plated OV cultures (Fig. 5A), as was BRN3, a POU-family transcription factor critical and specific for the development of ganglion cells (Fig. 5B).[22] By day 71, the relative percentage of BRN3+ retinal ganglion-like cells had diminished, presumably because of continued proliferation of NRPCs and production of other cell types (Fig. 5C). Also observed at day 39 and day 71 were cells expressing MAP2a/b (Figs. 5B, 5C), which is predominantly

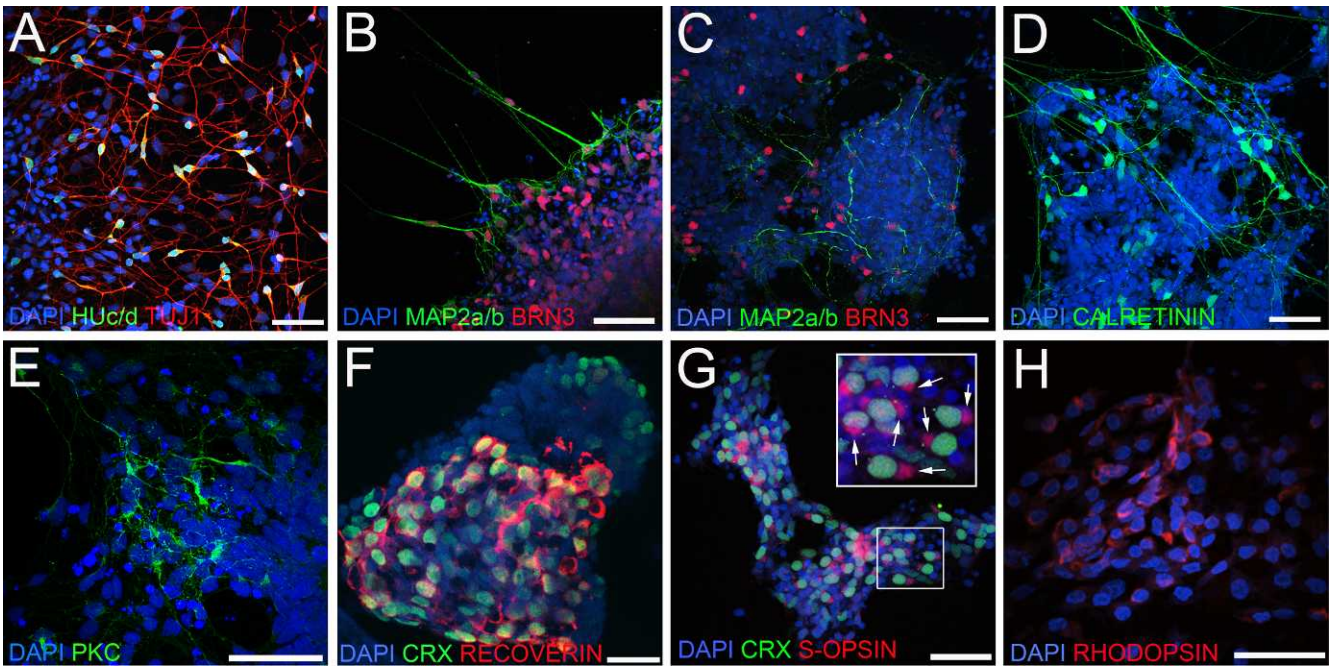

Figure 5. Differentiation of multiple neuroretinal cell types from TiPSC-OVs. (**A–F**) Immunocytochemistry analysis of partially dissociated, plated TiPSC-OVs was performed at various stages of differentiation. At day 39, postmitotic neuroretinal cells co-expressing (**A**) HUc/d and TUJ1 and (**B**) MAP2a/b and BRN3 were readily observed, the latter being indicative of ganglion-like cells. (**C**) BRN3+/MAP2a/b+ ganglion-like cells were also present later during differentiation (day 71 pictured), as were cells that expressed (**D**) CALRETININ (day 71 pictured) or (**E**) PKCα (day 77 pictured), markers of amacrine cells and ON bipolar cells in the human retina, respectively. (**F**) Many differentiated TiPSC-OV cells co-expressed the photoreceptor markers CRX and RECOVERIN at mid- to later stages of differentiation (day 108 pictured). (**G**) Co-expression of CRX and the cone-specific marker S-OPSIN was seen by day 78, with many of these cells exhibiting polarized expression of S-OPSIN (box inset, *arrows*). (**H**) At day 108, small clusters of cells expressed the rod photoreceptor gene RHODOPSIN, albeit diffusely throughout the cytoplasm. Scale bars = 50 μm.

expressed by ganglion cells, but also by horizontal cells and subsets of amacrine cells.[23] CALRETININ, which in the mature human retina is expressed in amacrine and ganglion cells,[24] was also present at day 71 (Fig. 5D). Other markers of retinal neurons were expressed around this time point as well, including PKCα (Fig. 5E), a signal transduction protein found in ON bipolar cells in the human retina.[25] Last, immunocytochemistry analysis revealed expression of photoreceptor markers, including CRX, RECOVERIN, S-OPSIN, and RHODOPSIN (Figs. 5F–H). Interestingly, we observed polarized expression of the cone photoreceptor marker S-OPSIN (Fig. 5G, inset), but not the rod photoreceptor marker RHODOPSIN (Fig. 5H).

Development of Primitive Retinal Laminae in Differentiating TiPSC-OVs

A recent study from Yoshiki Sasai's group demonstrated that laminated retina-like structures can spontaneously develop in differentiating mouse ESC cultures.[26] By sectioning and immunostaining intact TiPSC-OVs over time, we sought to determine whether differentiating hiPSC-derived retinal cell types had the capacity to self-assemble into higher-order structures as well.

As demonstrated previously for H9 hESC-OVs and IMR90-4 hiPSC-OVs,[7] TiPSC-OVs at day 20 were composed of radially oriented, proliferative CHX10+/Ki67+ NRPCs (Fig. 6A), reminiscent of the neuroblastic layer (NBL) within the developing human retina. By day 35, the Ki67+ proliferating NRPCs were predominantly located along the outer portion of the NBL-like region (Fig. 6B), whereas HUc/d+, TUJ1+, and BRN3+ postmitotic neurons congregated internally, forming a separate cell stratum that was CHX10–/Ki67– (Figs. 6B–E). These postmitotic neurons were primarily ganglion-like cells at this stage based on their co-expression of BRN3 and TUJ1 (Fig. 6D); however, CALRETININ+/BRN3– cells, indicative of amacrine cells, were also present within the presumptive ganglion cell layer (GCL) (Fig. 6E).

Between day 40 and day 70, most TiPSC-OVs lost their distinctive laminar appearance and developed internal rosettes, which contained a core of RECOVERIN+ photoreceptor-like cells surrounded by BRN3+/TUJ1+ ganglion-like cells (Fig. 6F); however, some TiPSC-OVs (16.8% ± 7.3%) retained areas of laminar structure long term. These areas became increasingly organized over time, eventually assuming a primitive, neuroretina-like appearance by immunocytochemistry (Figs. 6G–L). By day 72, three distinct cell laminae could be identified. CALRETININ+/BRN3– amacrine-like cells and CALRETININ+/BRN3+ ganglion-like cells were located in the innermost layer (Fig. 6G), followed by an intermediate layer containing primarily CHX10+ NRPCs (NBL; Fig. 6H), and an outer, thin layer of RECOVERIN+ photoreceptor-like cells (outer nuclear layer [ONL]; Figs. 6H, 6I). No MITF+ RPE cells were present in association with the neuroretinal laminae (data not shown). By day 105, the CHX10+ NBL and BRN3+ GCL were reduced in relative thickness, whereas the RECOVERIN+ ONL increased in thickness (Figs. 6J–L). PAX6 was confined to the inner and intermediate cell laminae at day 105, consistent with its expression in ganglion and amacrine cells (Fig. 6K). Although we observed a discontinuous separation between the GCL and NBL by nuclear staining at day 105 (asterisk in Figs. 6K, 6L), no clear inner plexiform layer was identified. Thus, despite our observation of multilaminar, neuroretina-like structures in differentiating TiPSC-OV cultures, modifications of the current system will likely be necessary to support development of more complex tissue architecture.

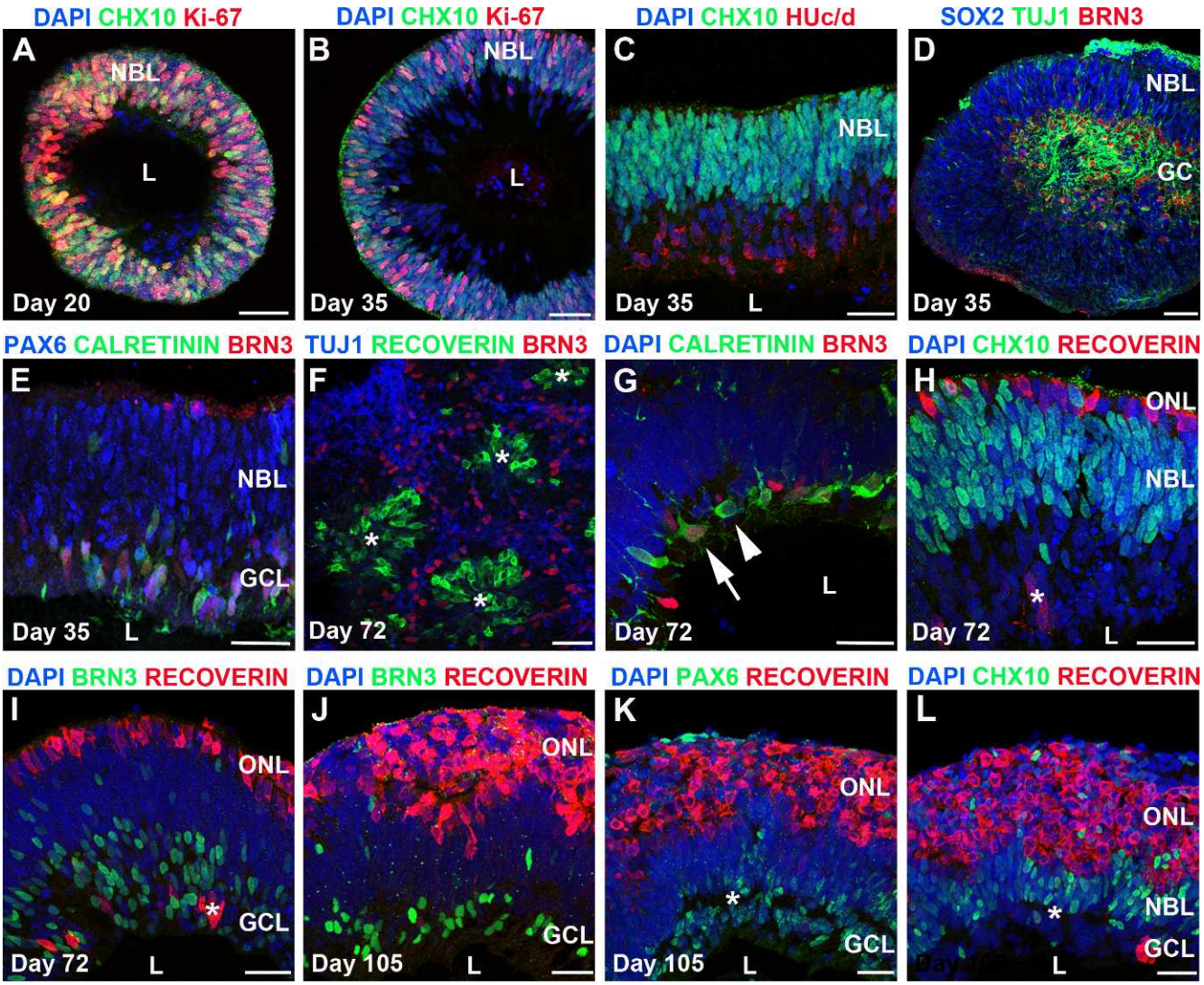

Figure 6. Self-assembly of TiPSC-OVs into multilayered retina-like structures. **(A-L)** Immunocytochemistry analysis of cryosectioned TiPSC-OVs at multiple stages of differentiation revealed regions that spontaneously organized into primitive retina-like tissues. (**A**) At day 20, most of the cells within TiPSC-OVs were mitotic NRPCs expressing CHX10 and Ki67. These radially oriented cells often surrounded an acellular lumen (L). (**B**) By day 35, an outer CHX10+/Ki67+ NBL remained; however, a layer of postmitotic CHX10– cells existed adjacent to the lumen. (**C**) HUc/d immunostaining confirmed the neuronal status of the postmitotic, CHX10– inner cell layer, which also contained numerous cells that (**D**) co-expressed BRN3 and TUJ1, resulting in its designation as a ganglion-like cell layer (GCL). In addition to being CHX10+, nuclei within the outer NBL at this stage were immunopositive for the NRPC marker SOX2. (**E**) PAX6 was highly expressed in both the NBL and GCL at day 35, whereas BRN3 and CALRETININ expression was confined to the GCL. (**F**) By day 72, laminar structure in TiPSC-OVs was often replaced by rosettes (*asterisks*); however, these rosettes retained some organization, with RECOVERIN+ photoreceptors located in the center surrounded by BRN3+/TUJ1+ ganglion-like cells. **(G-L)** Regions within TiPSC-OVs that did retain a laminar appearance continued to differentiate and self-assemble into more complex, multilayered neuroretina-like structures consisting of a putative ONL, an intermediate NBL, and an inner GCL. (**G**) By day 72 of differentiation, ganglion-like cells (BRN3+/CALRETININ+, *arrow*) could be discerned from amacrine-like cells (BRN3-/CALRETININ+, *arrowhead*) within the GCL. (**H**) The ONL, which was thin at day 72, contained RECOVERIN+ cells, whereas the NBL continued to harbor cells that expressed CHX10. Cells of the inner GCL were largely negative for these two markers, although occasional mislocalization of RECOVERIN+ cells was observed (*asterisk* in panels **H** and **I**). (**I**) Most nuclei in the GCL layer, adjacent to the lumen, continued to express BRN3. (**J–L**) By day 105, the putative RECOVERIN+ ONL had increased greatly in thickness, whereas the (**J**) BRN3+ GCL had proportionately thinned. (**K**) PAX6 expression was predominantly located in the GCL at this stage, although some expression was found in the NBL, which also contained (**L**) CHX10+ cells. There was a discontinuous gap between the NBL and GCL (*asterisk* in panels **K** and **L**); however, plexiform layers were not clearly evident (data not shown). Scale bars = 50 μm.

Synaptogenesis in TiPSC-OV–Derived Retinal Neurons

Although previous studies by our laboratory and others have demonstrated differentiation of retinal neurons from human induced pluripotent stem cells,[1,4–7] in vitro synaptogenesis has not been assessed in these cultures. In RT-PCR experiments, TiPSC-OV–derived retinal neurons upregulated genes necessary for synaptic transmission between day 20 and day 108 of differentiation (Fig. 7A). Critical presynaptic genes that were expressed included *VGLUT1*, the transporter responsible for loading glutamate into synaptic vesicles, and *SNAP-25,* which is required for formation of the SNARE complex. Postsynaptic receptor genes expressed during this period included *AMPA1*, *NMDA2A*, and retina-specific *MGLUR6. AMPA1* is relatively nonspecific within the retina, whereas *NMDA2A* is found in

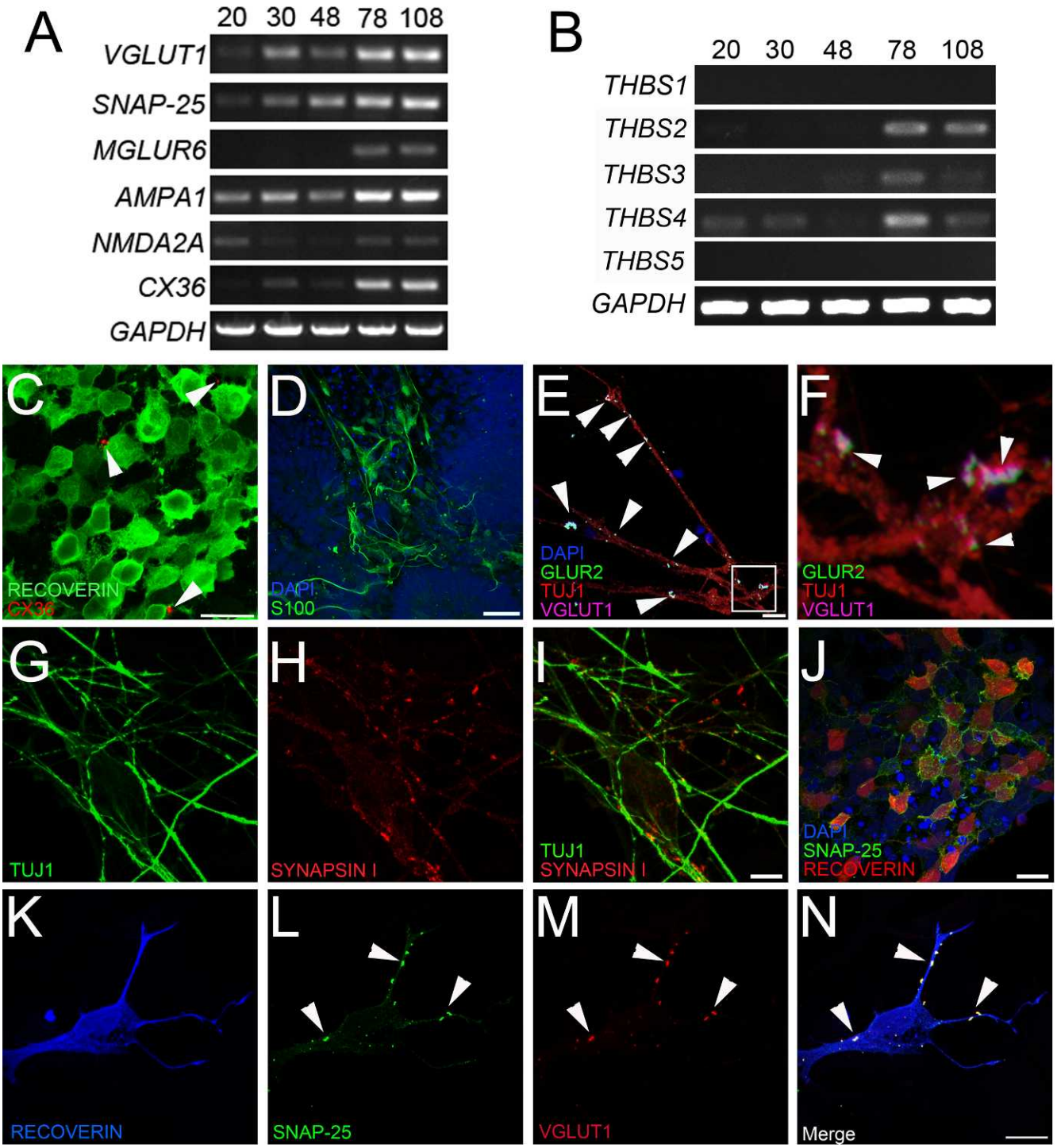

Figure 7. Expression of synaptic markers in TiPSC-OV cultures. (**A**) RT-PCR analysis revealed increased expression of presynaptic, postsynaptic, and gap junction (*CX36*) genes in TiPSC-OVs over time. (**B**) The thrombospondin genes *THBS2*, *3*, and *4*, which encode proteins known to promote synaptogenesis, were expressed in TiPSC-OVs by day 78. (**C–N**) Immunocytochemistry analysis of partially dissociated, plated TiPSC-OVs at day 78 of differentiation was performed to localize expression of synapse and gap junction proteins. (**C**) CX36 plaques were evident on RECOVERIN+ cells, although they were sparsely distributed (*arrowheads*). (**D**) S100 staining demonstrated the presence of glia, which support synaptic development, at day 78. (**E**) Low-magnification micrograph confirmed the presence of presynaptic VGLUT1 and postsynaptic GLUR2 along the processes of TUJ1+ neurons (*arrowheads*). (**F**) High magnification of the inset in panel **E**. VGLUT1+ punctae were adjacent to postsynaptic GLUR2+ punctae (*arrowheads*). (**G**) TUJ1+ neurites possessed numerous presynaptic (**H**) SYNAPSIN I punctae (merged image in panel **I**). (**J**) The presynaptic SNARE protein SNAP-25 was robustly expressed in RECOVERIN+ cells. (**K–N**) Image of a single (**K**) RECOVERIN+ photoreceptor-like cell with numerous punctae along its processes that co-expressed the presynaptic proteins (**L**) SNAP-25 and (**M**) VGLUT1. (**N**) Merged image of **K–M** showing nearly perfect colocalization of SNAP-25 and VGLUT1 (*arrowheads*). Scale bars for panels **C–J** = 20 μm; panels **K–N** = 10 μm.

retinal neurons making conventional synapses (ganglion and amacrine cells). *MGLUR6* was expressed at later stages of TiPSC-OV differentiation, coinciding with the expression of the ON bipolar marker, PKCα (Fig. 5E).

In addition to genes involved in chemical synaptic transmission, at least one required for the formation of electrical synapses, *CX36*, was upregulated over time in TiPSC-OV cultures (Fig. 7A). CX36 is a gap junction protein essential for visual processing in the adult retina, and is involved in several signaling pathways. CX36 expression has been verified in cones, AII amacrine cells, and ganglion cells, and may be present in gap junctions made by other retinal cell types as well.[27,28] In day 78 TiPSC-OV cultures, immunocytochemistry analysis revealed occasional CX36+ plaques on RECOVERIN+ photoreceptor-like cells (Fig. 7C).

Although thrombospondins perform an array of functions in different tissue types, within the central nervous system they are expressed by glia and are directly involved in neuronal synaptogenesis.[29] In differentiated TiPSC-OV cultures, *THBS2*, *3*, and *4* were upregulated late during differentiation (Fig. 7B), coinciding with expression of the glial marker S100 (Fig. 7D). Concurrent with the expression of *THBS* genes and S100, immunocytochemistry experiments revealed the presence of pre- and postsynaptic proteins on retinal neurons. To clearly identify their expression, TiPSC-OVs were partially dissociated and plated for 1 week before fixation and immunolabeling. Presynaptic VGLUT1 was consistently found juxtaposed to the postsynaptic glutamate receptor subunit GLUR2 on TUJ1+ neuronal processes (Figs. 7E, 7F), which were also decorated with punctate SYNAPSIN I staining (Figs. 7G–I). SYNAPSIN I is localized to the presynaptic terminals of neurons making conventional synapses (ganglion and amacrine cells), but not ribbon synapses (photoreceptors and bipolar cells).[30]

Synaptogenesis was also examined in RECOVERIN+ photoreceptor-like cells, which frequently expressed the presynaptic protein SNAP-25 on their surface (Fig. 7J). To more clearly assess co-expression of key presynaptic proteins on RECOVERIN+ photoreceptor-like cells, high-magnification imaging was performed. RECOVERIN+ cells clearly showed punctate VGLUT1 and SNAP-25 staining colocalized along the neuronal processes (Figs. 7K–N). These results demonstrate that retinal neurons produced by TiPSC-OVs have the capacity for cell-cell communication, and define the time frame of synapse and gap junction marker expression under our standard culture conditions.

Discussion

This study is the first to demonstrate production of multiple retinal cell types from blood-derived hiPSCs, and the first to report in vitro formation of stratified, neuroretina-like structures from any human pluripotent stem cell line. Furthermore, we established that retinal synapse markers are expressed in hiPSC cultures. Using a culture protocol previously established in our laboratory,[6,7] the peripheral blood T-lymphocyte TiPSC-5 cell line yielded OVs that were indistinguishable from those generated previously with hESCs and human fibroblast-derived iPS cell lines.[7] Over time, TiPSC-OVs produced numerous cell types with neuroretina-like phenotypes, including rod and cone photoreceptor-like cells. RPE was rarely seen in TiPSC-OVs, but was present in adherent TiPSC cultures, similar to all other human pluripotent stem cell lines we have tested. Thus, our differentiation method appears effective regardless of pluripotent stem cell origin.

For hiPSCs to be useful for regenerative medicine and disease modeling, the cell types they generate need to demonstrate functional potential. Our laboratory and others have shown that human pluripotent stem cell–derived retinal neurons display appropriate physiological properties in vitro.[5,7] In the present study, we extended those findings to include in vitro chemical and electrical synapse formation. TiPSC-OV–derived TUJ1+ neurons and RECOVERIN+ photoreceptor-like cells expressed several proteins required for neurotransmitter release, including VGLUT1 and SNAP-25. Furthermore, TUJ1+ neurons were predominantly SYNAPSIN I+, identifying them as amacrine-like or ganglion-like cells. The presence of synapses on TUJ1+ neurites was suggested by the close apposition of presynaptic VGLUT1 and postsynaptic GLUR2, the latter being a subunit of ionotropic AMPA (alpha-amino-3-hydroxy-5-methyl-4isoxazole-propionic acid) glutamate receptors expressed in both the outer and inner plexiform layers of the primate retina.[31] We also documented upregulation of *MGLUR6*, a postsynaptic glutamate receptor gene expressed exclusively in retinal ON bipolar cells. Of note, while the present study is the first to document retinal synaptic marker expression in hiPSCs, SYNAPTOPHYSIN expression was previously demonstrated on INTERNEXIN+ retinal neurons in hESC culture.[32]

In vitro, the formation and maintenance of functional synapses is greatly facilitated by the presence of glia.[32] Recently, one of the synaptogenic factors secreted from glia was identified: a conserved domain common to all thrombospondin isoforms.[29] In differentiating TiPSC-OVs, the timing of thrombospondin gene expression coincided with the appearance of both synapses and glia. Although the temporal expression of thrombospondin isoforms is suggestive of a role in synaptogenesis, further studies are needed to confirm the source and function of thrombospondins in retinal cultures derived from hiPSCs.

In addition to chemical synapses, the presence of gap junctions is vital for cell-cell communication throughout the neural retina. Gap junctions are formed by a variety of connexins, but CX36 is perhaps the most important, particularly for transmission of the rod signal.[27,33,34] To our knowledge, this is the first report of CX36 expression in retinal progeny of human pluripotent stem cell cultures; however, the sparse distribution of CX36 plaques on RECOVERIN+ photoreceptor-like cells suggests that further maturation and/or changes in culture conditions are needed to fully promote gap junction formation in vitro. Even so, these data suggest that TiPSC-OV cultures may be useful for studying synapse development and/or generating donor retinal neurons capable of communicating with host cells following transplantation into the subretinal space.

Beyond demonstrating synaptogenic potential, an ideal hiPSC- or hESC-based retinal model system would maintain appropriate spatial relationships between neuroretinal cell types. Recently, Eiraku et al.[26] showed that mouse ESCs could form bilayered optic cups composed of an outer layer of Mitf+ presumptive RPE and an inner layer of proliferating Chx10+ NRPCs. Subsequently, the NRPC layer self-organized into a multilayered structure that closely resembled the developing murine retina. Similarly, sectioning and immunostaining of TiPSC-OVs revealed areas of discernible outer, intermediate, and inner cell layers populated by photoreceptor-like cells, retinal progenitors, and ganglion-like cells, respectively. The overall degree of spontaneous retinal organization we observed with human TiPSCs was primitive in comparison with that described by Eiraku et al.[26] using mouse ESCs; however, our culture methods differed considerably. We cultured OVs in large batches and did not use high-oxygen, Matrigel, retinoic acid, or Notch inhibitors, nor was RPE present. The absence of these and other influences may explain some of the limitations of our current system, but it also provides insight into the innate ability of human NRPCs and their progeny to self-assemble during differentiation. Future experiments will seek

to delineate circumstances that promote neuroretinal laminae formation in vitro, with the hope of improving efficiency and extending our findings across multiple human pluripotent stem cell lines.

Taken together, our results establish TiPSCs as a potentially valuable source of pluripotent stem cells for in vitro studies of human retinal development and disease. In addition, transplantation of TiPSC-derived neuroretinal tissue-like populations may prove useful for the treatment of advanced retinal degenerative diseases, provided that safety and efficacy can be established and the host ganglion cell layer remains at least partially intact. Toward ensuring safety, methods now exist to generate integration-free hiPSCs from routine peripheral blood samples.[35] To demonstrate efficacy, significant hurdles must be overcome, including the need to translate our findings in OV cultures to a platform suitable for subretinal transplantation. Once achieved, efforts will be directed toward testing tissue-like sheets of human neuroretinal cells (± RPE) derived from hiPSCs in rodent models of retinal degenerative diseases.

References

1. Lamba DA, McUsic A, Hirata RK, Wang PR, Russell D, Reh TA. Generation, purification and transplantation of photoreceptors derived from human induced pluripotent stem cells. *PLoS One*. 2010;5:e8763.
2. Lamba DA, Gust J, Reh TA. Transplantation of human embryonic stem cell-derived photoreceptors restores some visual function in Crx-deficient mice. *Cell Stem Cell*. 2009;4:73–79.
3. Osakada F, Ikeda H, Mandai M, et al. Toward the generation of rod and cone photoreceptors from mouse, monkey and human embryonic stem cells. *Nat Biotechnol*. 2008;26:215–224.
4. Hirami Y, Osakada F, Takahashi K, et al. Generation of retinal cells from mouse and human induced pluripotent stem cells. *Neurosci Lett*. 2009;458:126–131.
5. Jin ZB, Okamoto S, Osakada F, et al. Modeling retinal degeneration using patient-specific induced pluripotent stem cells. *PLoS One*. 2011;6:e17084.
6. Meyer JS, Shearer RL, Capowski EE, et al. Modeling early retinal development with human embryonic and induced pluripotent stem cells. *Proc Natl Acad Sci U S A*. 2009;106:16698–16703.
7. Meyer JS, Howden SE, Wallace KA, et al. Optic vesicle-like structures derived from human pluripotent stem cells facilitate a customized approach to retinal disease treatment. *Stem Cells*. 2011;29:1206–1218.
8. Lu B, Malcuit C, Wang S, et al. Long-term safety and function of RPE from human embryonic stem cells in preclinical models of macular degeneration. *Stem Cells*. 2009;27:2126–2135.
9. Rowland TJ, Buchholz DE, Clegg DO. Pluripotent human stem cells for the treatment of retinal disease. *J Cell Physiol*. 2012;227:457–466.
10. Sugino IK, Sun Q, Wang J, et al. Comparison of FRPE and human embryonic stem cell-derived RPE behavior on aged human Bruch's membrane. *Invest Ophthalmol Vis Sci*. 2011;52:4979–4997.
11. Howden SE, Gore A, Li Z, et al. Genetic correction and analysis of induced pluripotent stem cells from a patient with gyrate atrophy. *Proc Natl Acad Sci U S A*. 2011;108:6537–6542.
12. Buchholz DE, Hikita ST, Rowland TJ, et al. Derivation of functional retinal pigmented epithelium from induced pluripotent stem cells. *Stem Cells*. 2009;27:2427–2434.
13. Carr AJ, Vugler AA, Hikita ST, et al. Protective effects of human iPS-derived retinal pigment epithelium cell transplantation in the retinal dystrophic rat. *PLoS One*. 2009;4:e8152.
14. Chen M, Chen Q, Sun X, et al. Generation of retinal ganglion-like cells from reprogrammed mouse fibroblasts. *Invest Ophthalmol Vis Sci*. 2010;51:5970–5978.
15. Parameswaran S, Balasubramanian S, Babai N, et al. Induced pluripotent stem cells generate both retinal ganglion cells and photoreceptors: therapeutic implications in degenerative changes in glaucoma and age-related macular degeneration. *Stem Cells*. 2010;28:695–703.
16. Tucker BA, Park IH, Qi SD, et al. Transplantation of adult mouse iPS cell-derived photoreceptor precursors restores retinal structure and function in degenerative mice. *PLoS One*. 2011;6:e18992.
17. Zhou L, Wang W, Liu Y, et al. Differentiation of induced pluripotent stem cells of Swine into rod photoreceptors and their integration into the retina. *Stem Cells*. 2011;29:972–980.
18. Hu Q, Friedrich AM, Johnson LV, Clegg DO. Memory in induced pluripotent stem cells: reprogrammed human retinal-pigmented epithelial cells show tendency for spontaneous redifferentiation. *Stem Cells*. 2010;28:1981–1991.
19. Brown ME, Rondon E, Rajesh D, et al. Derivation of induced pluripotent stem cells from human peripheral blood T lymphocytes. *PLoS One*. 2010;5:e11373.
20. Takahashi K, Tanabe K, Ohnuki M, et al. Induction of pluripotent stem cells from adult human fibroblasts by defined factors. *Cell*. 2007;131:861–872.
21. Yu J, Vodyanik MA, Smuga-Otto K, et al. Induced pluripotent stem cell lines derived from human somatic cells. *Science*. 2007;318:1917–1920.
22. Mu X, Klein WH. A gene regulatory hierarchy for retinal ganglion cell specification and differentiation. *Semin Cell Dev Biol*. 2004;15:115–123.
23. Tucker RP, Matus AI. Microtubule-associated proteins characteristic of embryonic brain are found in the adult mammalian retina. *Dev Biol*. 1988;130:423–434.
24. Nag TC, Wadhwa S. Developmental expression of calretinin immunoreactivity in the human retina and a comparison with two other EF-hand calcium binding proteins. *Neuroscience*. 1999;91:41–50.
25. Haverkamp S, Haeseleer F, Hendrickson A. A comparison of immunocytochemical markers to identify bipolar cell types in human and monkey retina. *Vis Neurosci*. 2003;20:589–600.
26. Eiraku M, Takata N, Ishibashi H, et al. Self-organizing optic-cup morphogenesis in three-dimensional culture. *Nature*. 2011;472:51–56.
27. Bloomfield SA, Volgyi B. The diverse functional roles and regulation of neuronal gap junctions in the retina. *Nat Rev Neurosci*. 2009;10:495–506.
28. Pan F, Paul DL, Bloomfield SA, Volgyi B. Connexin36 is required for gap junctional coupling of most ganglion cell subtypes in the mouse retina. *J Comp Neurol*. 2010;518:911–927.
29. Christopherson KS, Ullian EM, Stokes CC, et al. Thrombospondins are astrocyte-secreted proteins that promote CNS synaptogenesis. *Cell*. 2005;120:421–433.
30. Mandell JW, Townes-Anderson E, Czernik AJ, Cameron R, Greengard P, De Camilli P. Synapsins in the vertebrate retina: absence from ribbon synapses and heterogeneous distribution among conventional synapses. *Neuron*. 1990;5:19–33.
31. Grunert U, Haverkamp S, Fletcher EL, Wassle H. Synaptic distribution of ionotropic glutamate receptors in the inner plexiform layer of the primate retina. *J Comp Neurol*. 2002;447:138–151.
32. Lamba DA, Karl MO, Ware CB, Reh TA. Efficient generation of retinal progenitor cells from human embryonic stem cells. *Proc Natl Acad Sci U S A*. 2006;103:12769–12774.

33. Sohl G, Joussen A, Kociok N, Willecke K. Expression of connexin genes in the human retina. *BMC Ophthalmol*. 2010; 10:27.
34. Hansen KA, Torborg CL, Elstrott J, Feller MB. Expression and function of the neuronal gap junction protein connexin 36 in developing mammalian retina. *J Comp Neurol*. 2005;493:309–320.
35. Rajesh D, Dickerson SJ, Yu J, Brown ME, Thomson JA, Seay NJ. Human lymphoblastoid B-cell lines reprogrammed to EBV-free induced pluripotent stem cells. *Blood*. 2011;118:1797–1800.